Synergistic Effect of Molybdate and Zn^{2+} on the Inhibition of Corrosion of Mild Steel in Neutral Aqueous Environment

S. Rajendran*, B.V. Apparao and N. Palaniswamy*****

* *Department of Chemistry, G.T.N. Arts College (Automomous), DINDIGUL - 624 005 India*

** *Department of Chemistry, Regional Engineering College, WARANGAL 506 004*

*** *Corrosion Science and Engineering Division, CECRI, KARAIKUDI 630 006*

The synergistic effect of molybdate and Zn^{2+} on the inhibition of corrosion of mild steel in neutral aqueous environment containing 60 ppm Cl^- has been evaluated by the weight-loss method. The mechanistic aspects of corrosion inhibition have been studied, in a holistic way, using potentiostatic polarisation study, X-ray diffraction technique, uv-visible reflectance and luminescence spectra. The formulation consisting of 300 ppm molybdate and 50 ppm Zn^{2+} has 90% corrosion inhibition efficiency. The protective film consists of ferric molybdate, zinc peroxide and γ-FeOOH. This film is found to be semiconducting and luminescent.

Molybdate anion has been widely used as corrosion inhibitor since 1939, because of its efficacy towards both ferrous and non-ferrous metal and its very low order of toxicity. Molybdate has been used as inhibitor in combination with nitrite [1-3], alkyl amine phosphonate [4-6] and azoles like benzotrizole and tolyltriazole [7]. Eventhough several studies have been reported on the synergistic effect of molybdate-zinc system [6,8-10], the mechanistic aspects have not been studied in detail. In the present study, the synergistic effect of molybdate and Zn^{2+}, on the inhibition of corrosion of mild steel in neutral aqueous environment containing 60 ppm Cl^- has been evaluated by the weight-loss method; the mechanism of corrosion inhibition has been studied using potentiostatic polarisation study, X-ray diffraction (XRD) technique, uv-visible and luminescence spectra.

EXPERIMENTAL

Preparation of the Specimens

Mild steel (0.02 to 0.03% S, 0.03 to 0.08% P, 0.4 to 0.5% Mn, 0.1 to 0.2% C and the rest iron) was used in this study. Specimens of dimensions 1 x 4 x 0.2 cm were used for the weight-loss method and surface examination studies. Mild steel rod (encapsulated in Teflon with an exposed cross section of 0.5 cm diameter) was used as the working electrode in potentiostatic polarisation studies. Surface of both specimens were polished to mirror finish and degreased with trichloroethylene before use.

© E.C.S.I. Bangalore

Weight-loss Method

Weight-loss studies were carried out in presence of different concentration of inhibitor in the absence and presence of Zn^{2+} by immersing the mild steel specimens in 100 ml of various media for a period of seven days . The weights of the specimens before and after immersion were determined using Mettler balance, AE-240. Measurements were made in triplicate.

Potentiostatic Polarisation Study

This study was carried out in a three electrode cell assembly (mild steel, platinum and SCE) connected to an electrochemical analyser provided with IR compensation facility (of Bioanalytical system model BAS - 100 A).

Surface Examination Study

The mild steel specimens were immersed in various test solutions for a period of two days. After two days, the specimens were taken out and dried. The nature of the film formed on the surface of the metal specimens was analysed by various surface analysis techniques.

The uv-visible Spectra

The uv-visible reflectance spectra were recorded using Hitachi U-3400 spectrophotometer.

X-ray Diffraction Technique

The XRD patterns of the film formed on the metal surface were recorded using a computer controlled X-ray powder diffractometer, JEOL JDX 8030 with CuK_α (Ni-filtered) radiation (λ = 15.418 nm) at a rating of 40 kV, 20 mA. The scan rate was 0.05-20° per step and the measuring time was 1 second per step.

Luminescence Spectra

The luminescence spectra of the film formed on the metal surface were recorded using Hitachi 650-10 S fluorescence spectrophotometer equipped with 15 W Xenon lamp and a Hamamatsu R 928 F photomultiplier tube. The emission spectra were corrected for the spectral response of the photomultiplier tube used and the excitation spectra recorded were corrected for the beam intensity variation.

RESULTS AND DISCUSSION

Weight-loss Method

The corrosion rates of mild steel in neutral aqueous environment containing 60 ppm chloride, in the absence and presence of inhibitors obtained by the weight-loss method are given in Table 1. The corrosion inhibition efficiencies of various systems are also given in Table 1.

It is envident from Table 1 that 300 ppm MoO_4^{2-} has 80% inhibition efficiency and 50 ppm Zn^{2+} is found to be corrosive. However, the formulation consisting of 300 ppm MoO_4^{2-} and 50 ppm Zn^{2+} has 90% inhibition efficiency. This indicates the synergistic effect between molybdate anion and Zn^{2+}.

Potentiostatic Polarisation Study

The potentiostatic polarisation curves of mild steel immersed in various environments are given in Fig. 1. It may be noted that 50 ppm Zn^{2+} alone shifts the corrosion potential to the cathodic side (from -389 mV to -489 mV *vs* SCE). 300 ppm MoO_4^{2-} alone shifts the corrosion potential to the anodic side

Table 1

Corrosion rates of mild steel and the inhibition efficiencies obtained by the weight-loss method.

Inhibitor system : MoO_4^{2-} + Zn^{2+}
Medium: Neutral aqueous environment containing Cl^- = 60 ppm in the absence and presence of inhibitor

MoO_4^{2-} ppm	Zn^{2+} ppm	Corr.rate mdd	Inhib.eff. %
0	0	15.54	-
0	50	19.11	-23
300	-	3.11	80
300	50	1.58	90

(from -389 mV to -295 mV). In the presence of 300 ppm MoO_4^{2-} and 50 ppm Zn^{2+} together, the corrosion potential is shifted to -304 mV *vs* SCE. This potential is in between that of MoO_4^{2-} alone and Zn^{2+} alone. This indicates that this formulation acts as a mixed inhibitor. This is further supported by the fact that the MoO_4^{2-} - Zn^{2+} combination shifts both the anodic and cathodic slopes almost equally to the extent of 25 mV/decade.

UV-visible Reflectance Spectra

The uv-visible reflectance spectra of the film formed on the surface of the metal specimens immersed in various test solutions are given in Fig. 2. The uv-visible reflectance spectra of the unpolished metal, of the polished metal immersed in the environment containing 60 ppm Cl^- and that of the polished

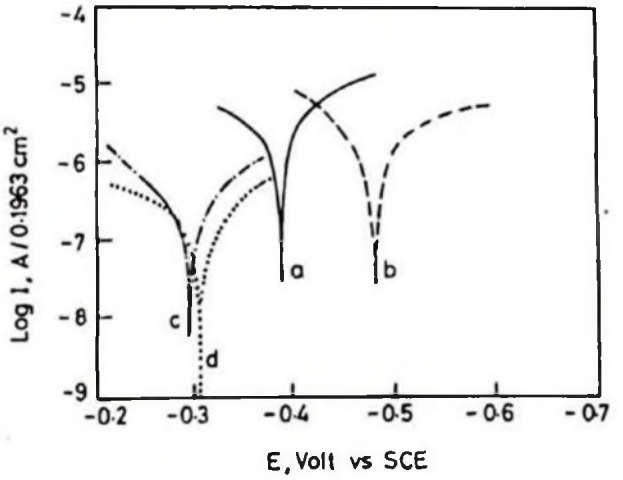


Fig. 1. Potentiostatic polarisation curves of mild steel immersed in various environments

(a) Cl^- 60 ppm
(b) Cl^- 60 + Zn^{2+} 50 ppm
(c) Cl^- 60 + MoO_4^{2-} 300 ppm
(d) Cl^- 60 + MoO_4^{2-} 300 + Zn^{2+} 50 ppm

metal immersed in the environment consisting of 60 ppm Cl^- and 50 ppm Zn^{2+} show wavelength transition at 550 nm revealing that the band gap (E_g) of the film formed on the above surfaces is 1.239/0.55 = 2.25 eV. This suggests that the film formed on the above surfaces consists of oxides of iron [11-14] having semiconducting property [15-18].

On the other hand, the uv-visible reflectance spectrum of the polished metal (Fig. 2b) does not show any wavelength transition at 550 nm. That is because, this surface is free from any oxides of iron.

The reflectance spectrum of the film due to the environment containing 60 ppm Cl^- and 300 ppm MoO_4^{2-} (Fig. 2e) has a peak at 320 nm. This may be due to the presence of iron-molybdate complex formed on the metal surface. The uv-visible reflectance spectrum of the film due to the environment consisting of 60

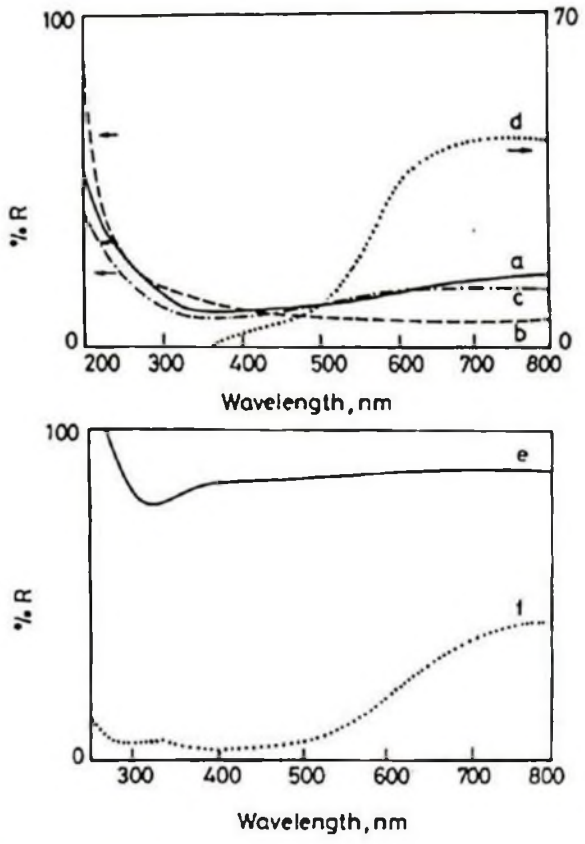


Fig.2. UV-visible reflectance spectra of mild steel surface immersed in various environments

(a) unpolished metal (b) polished metal
(c) Cl^- 60 ppm
(d) Cl^- 60 + Zn^{2+} 50 ppm
(e) Cl^- 60 + MoO_4^{2-} 300 ppm
(f) Cl^- 60 + MoO_4^{2-} 300 + Zn^{2+} 50 ppm

ppm Cl^-, 300 ppm MoO_4^{2-} and 50 ppm Zn^{2+} shows wave length transition at 550 nm indicating the presence of oxides of iron [11-14] having semiconducting property [15-18]. The peak at 320 nm may be due to iron molybdate complex.

X-ray Diffraction Patterns

The X-ray diffraction (XRD) patterns of the films formed on the surfaces of the metal specimens immersed in various test solutions are given in Fig. 3. The surface of the unpolished metal contains γ FeOOH (2θ - 13.6°), Fe_3O_4 (2θ - 35.7°) and α-FeOOH (2θ - 58.2°). The peak due to iron occurs at 2θ = 44.2° [19].

In the case of polished metal, the peaks due to iron appear at 2θ = 44.8°, 65.1°, 82.4° and 99.0°. When the metal

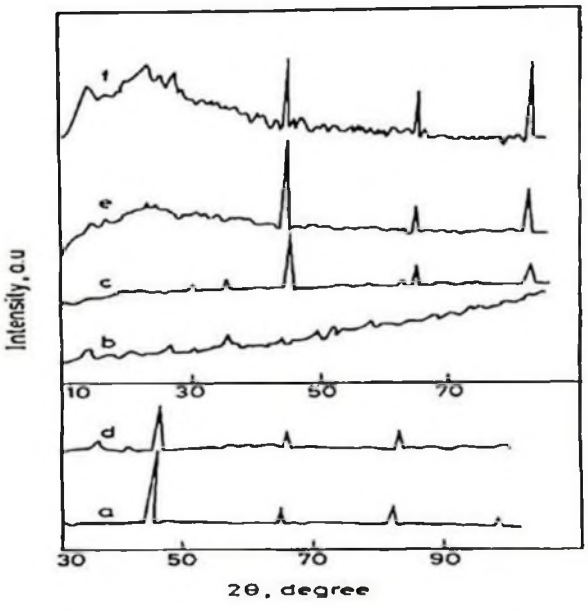


Fig. 3. XRD patterns of mild steel surface immersed in various environments

(a) polished metal (b) unpolished metal
(c) Cl^- 60 ppm
(d) Cl^- 60 + Zn^{2+} 50 ppm
(e) Cl^- 60 + MoO_4^{2-} 300 ppm
(f) Cl^- 60 + MoO_3^{2-} 300 + Zn^{2+} 50 ppm

specimen is immersed in 60 ppm Cl^- solution, iron peaks do appear; in addition, peaks due to magnetite (Fe_3O_4) occur at 2θ = 30.1°, 35.5° and 62.5° [19]. This indicates that in the chloride environment, mild steel specimen has undergone corrosion leading to the formation of magnetite.

The XRD pattern of the surface of the metal immersed in the solution

containing 60 ppm Cl^- and 50 ppm Zn^{2+} is given in Fig. 3d. It suggests the presence of Fe_3O_4 (2θ = 35.4°). The peaks due to iron occur at 2θ = 44.8°, 65.1° and 82.5° [19].

The XRD pattern of the film due to the environment containing 60 ppm Cl^- and 300 ppm MoO_4^{2-} suggests the presence of $Fe_2(MoO_4)_3$ on the metal surface (2θ = 14.1°, 22.6°, 30.63° and 31.88°) [20]. The peaks due to iron appear at 2θ = 44.5°, 64.8° and 82.2°.

The film formed on the surface of the mild steel specimen immersed in the environment consisting of 60 ppm Cl^-, 300 ppm MoO_4^{2-} and 50 ppm Zn^{2+} consists of $Fe_2(MoO_4)_3$ (2θ = 22.0°, 26.7°, 45.5° and 66.1°) [20], ZnO_2 (2θ = 45.5° and 66.1°) [21] and γFeOOH (2θ = 60.9°) [19]. The iron peaks appear at 2θ = 44.6°, 65.0° and 82.3°.

Analysis of the Luminescence Spectra

The emission spectrum (λ_{ex} = 300 nm) of the film formed on the surface of the metal immersed in the environment consisting of 60 ppm Cl^- and 300 ppm MoO_4^{2-} is given in Fig. 4a. This spectrum is probably due to $Fe_2(MoO_4)_3$. The corresponding excitation spectrum (λ_{em} = 420 nm) is given in Fig. 4c.

The emission spectrum (λ_{ex} = 300 nm) of the film due to the environment containing 60 ppm Cl^-, 300 ppm MoO_4^{2-} and 50 ppm Zn^{2+} is given in Fig. 4b. This spectrum is probably due to $Fe_2(MoO_4)_3$ embedded in γFeOOH and ZnO_2. The corresponding excitation spectrum (λ_{em} = 440 nm) is given in Fig. 4d.

It is found that in the presence of Zn^{2+}, the intensity of the peaks increases in

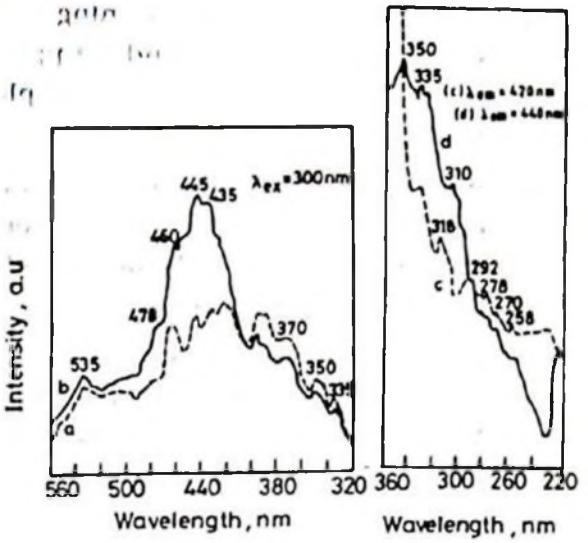


Fig. 4. Luminescence spectra of mild steel surface immersed in various environments

(a) and (c) Cl 60 + MoO_4^{2} 300 ppm
(b) and (d) Cl 60+MoO_4^{2} 300 + Zn^{2+} 50 ppm

the region of 400 to 560 nm (cf. Fig. 4a and b). The formation of $Fe_2(MoO_4)_3$ on the metal surface appears to be enhanced in the presence of Zn^{2+} in the environment.

Mechanism of Corrosion Inhibition

Results of the weight-loss method reveal that the formulation consisting of 300 ppm molybdate and 50 ppm Zn^{2+} has 90% inhibition efficiency. Potentiostatic polarisation study shows that this formulation acts as mixed inhibitor. The uv-visible reflectance spectrum suggests that the protective film contains iron-molybdate complex and oxides of iron having semiconducting property. The XRD technique indicates that the protective film consists of $Fe_2(MoO_4)_3$, ZnO_2 and γ-FeOOH. The protective film is found to be luminescent. In order to explain all these observed facts in a holistic way, the following mechanism of corrosion inhibition is proposed.

1. When the medium containing 60 ppm Cl^-, 300 ppm MoO_4^{2-} and 50 ppm Zn^{2+} is prepared, Zn^{2+}-MoO_4^{2-} complex is formed in solution.
2. When the metal is immersed in this environment, the Zn^{2+}-MoO_4^{2-} complex diffuses from the bulk of the solution to the surface of the metal.
3. On the surface of the metal, Zn^{2+} - MoO_4^{2-} complex is converted into Fe^{3+}-MoO_4^{-2} complex on the local anodic sites, as the latter is more stable than the former.

   $$3\ Zn^{2+} - MoO_4^{2-} + 2\ Fe^{3+} \longrightarrow Fe_2(MoO_4)_3 + 3\ Zn^{2+}$$

4. The released Zn^{2+} ions on the surface form $Zn(OH)_2$. There is formation of γ-FeOOH also on the cathodic sites.

This explains the presence of $Fe_2(MoO_4)_3$, ZnO_2 and γ-FeOOH in the protective film.

CONCLUSION

In the absence of Zn^{2+}, the protective film consists of $Fe_2(MoO_4)_3$ only and does not contain any oxides of iron. This film is not semiconducting but luminescent. MoO_4^{2-} acts as the anodic inhibitor and offers 80% inhibition.

The formulation containing both together acts as a mixed inhibitor. The protective film is semiconducting & luminescent; it consists of $Fe_2(MoO_4)_3$, ZnO_2 and γ-FeOOH.

ACKNOWLEDGEMENT

S.R. is thankful to Mr. Ranjit Soundarajan, the Correspondent, Prof. S. Ramakrishnan, the Principal and Prof. P. Jayaram, H.O.D. of Chemistry, G.T.N. Arts College (Autonomous), Dindigul for their encouragement and to the University Grants Commission, New Delhi, India for awarding a Fellowship.

REFERENCES

1. A.L. Bayes, **US Patent 2,147,395** (1939).
2. D.R. Robitaille, *Materials Performance*, **15(11)** (1976) 40.
3. F.C. Sessa and R.M. Post, *The Betz Indicator*, **52(3)** (1981) 9.
4. R.J. Lipinski and R.F. Weidner, *Heating/Piping/Air Conditioning*, **50(1)** (1978) 103.
5. T.C. Breske, *Materials Performance*, **16(2)** (1977) 17.
6. D.R. Robitaille and J.G. Blick, *Chem. Eng.*, **83(12)** (1976) 79.
7. C.O' Neal, Jr., R.N. Borger, *Materials Performance.*, **15(2)** (1976) 9.
8. M.A. Stranick, *Proc. 4th Intl. Conf. Chemistry and Uses of Molybdenum*, **AMAX Inc., Greenwich, CT**, August (1982) 123.
9. D.M. Drazic and L.Z. Vorkapic, *Corrosion Science*, **18** (1978) 907.
10. M.S. Vukasovich and D.R. Robitaille, *J.Less Common Metals*, **54** (1977) 437.
11. M. Sharon, G. Tamizhmani and K. Basaraswaram, *Proc. Indian Nat. Sci. Acad.*, **52** (1986) 311.
12. H.L. Sanchez, H. Steinfink and H.S. White, *J. Solid State Chem.*, **41** (1982) 90.
13. M. Sharon and B.M. Prasad, *Solar Energy Mat.*, **8** (1983) 457.
14. C. Sanchez, K.D. Sieber and G.A. Somorjai, *J. Electroanal. Chem.*, **252** (1988) 269.
15. W. Schultze and U. Stimming, *Z. Phys. Chem. N.F.*, **98** (1975) 285.
16. S.M. Wilhelm, K.S. Yun, L.W. Ballenger and N. Hackerman, *J. Electrochem. Soc.*, **126** (1979) 416.
17. S.M. Wilhelm and N. Hackerman, *J. Electrochem. Soc.*, **128** (1981) 1668.
18. L.M. Abrantes and L.M. Peter, *J. Electroanal. Chem.*, **150** (1983) 593.
19. M. Favre and D. Landolt, *Corrosion Science*, **34** (1993) 1481.
20. JCPDS Nr. 200526.
21. JCPDS Nr. 130311.